Arabian Journal of Chemistry (2021) **14**, 103083

King Saud University

Arabian Journal of Chemistry

www.ksu.edu.sa
www.sciencedirect.com

ORIGINAL ARTICLE

Zinc nanoparticles green-synthesized by *Alhagi maurorum* leaf aqueous extract: Chemical characterization and cytotoxicity, antioxidant, and anti-osteosarcoma effects

Arunachalam Chinnathambi [a,*], **Tahani Awad Alahmadi** [b]

[a] *Department of Botany and Microbiology, College of Science, King Saud University, Riyadh 11451, Saudi Arabia*
[b] *Department of Pediatrics, College of Medicine, King Saud University, King Khalid University Hospital, PO Box-2925, Riyadh 11461, Saudi Arabia*

Received 10 January 2021; accepted 10 February 2021
Available online 22 February 2021

KEYWORDS

Zinc nanoparticles;
Chemical characterization;
Alhagi maurorum leaf;
Anti-human osteosarcoma cancer;
Antioxidant;
Cytotoxicity

Abstract In this study, zinc oxide nanoparticles (ZnONPs) were synthesized in an aqueous medium using the plant extract as stabilizing and reducing agents. The synthesized ZnONPs were characterized using different techniques including Ultraviolet–visible (UV–Vis) and Fourier-transform infrared (FTIR) spectroscopy, X-ray diffraction (XRD), scanning electron microscopy (SEM), and Energy Dispersive X-ray Spectrometry (EDS). According to the XRD analysis, 21.46 was measured for ZnONPs crystal size. SEM images exhibited a uniform spherical morphology in size of 27.92 nm for the biosynthesized nanoparticles respectively. For evaluating anti-osteosarcoma and cytotoxicity effects of ZnONPs, $Zn(NO_3)_2{\cdot}6H_2O$, and *Alhagi maurorum* aqueous extract, we used 3-(4,5-dimethylthiazol-2-yl)-2,5-diphenyl-2H-tetrazolium bromide (MTT) assay. The result of this test showed that ZnONPs have no cytotoxicity on normal cell line (Human umbilical vein endothelial cells (HUVECs)) and have potent anti-osteosarcoma features dose-dependently against G-292, clone A141B1, MG-63, HOS, Hs 707(A).T, and Saos-2 cell lines. For evaluating the antioxidant features of ZnONPs, $Zn(NO_3)_2{\cdot}6H_2O$, and *Alhagi maurorum* aqueous extract, we used the 2,2-diphenyl-1-picrylhydrazyl (DPPH) test, in this test butylated hydroxytoluene was a positive control, the results of this test showed that the ZnONPs have an effective antioxidant feature. Probably,

* Corresponding author.
E-mail address: carunachalam@ksu.edu.sa (A. Chinnathambi).
Peer review under responsibility of King Saud University.

Production and hosting by Elsevier

https://doi.org/10.1016/j.arabjc.2021.103083

potent anti-human osteosarcoma activities of ZnONPs formulated with *Alhagi maurorum* aqueous seed extract because of antioxidant properties.

1. Introduction

Chemotherapeutic drugs including Methotrexate, Doxorubicin (Adriamycin), Cisplatin or carboplatin, Epirubicin, Ifosfamide, Cyclophosphamide, Etoposide, Gemcitabine, and Topotecan are common drugs for treating several types of cancers especially osteosarcoma (Bone cancer). According to the high side effects of chemotherapeutic drugs such as weight loss, mouth sores, vomiting, diarrhea, hair loss, fatigue, and nausea, the formulation of modern chemotherapeutic drugs is necessary (Sharma et al., 2017). Scientists understood that metallic nanoparticles have excellent anticancer properties, from past to present (Zangeneh, 2019; Mohammadi et al., 2019). Recent experimental studies have shown that some nanoparticles (with metal content) with different physicochemical properties have begun to offer new possibilities for treating various diseases (Mahdavi et al., 2019a,b; Ghaneialvar et al., 2019; Goorani et al., 2020).

Nowadays, nanotechnology has been developed in several ways due to its wide range of applications. The surface area to volume ratio of nanoparticles makes them potent agents in biological aspects (Moradi et al., 2019; Rashidi et al., 2018; Sherkatolabbasieh et al., 2017). Nanomaterials have better physicochemical features than their counterparts, some of these features are as follows: optical, toxicity, color, prevalence, solubility, strength, thermodynamics, magnetic, etc (Zhaleh et al., 2018; Zangeneh et al., 2019). Metallic nanoparticles with various properties and a wide range of activity have been well known (Jalalvand et al., 2019; Zhaleh et al., 2019). The present time's biological methods that are eco-friendly, non-toxic, and cost-effective have been developed for the synthesis of nanoparticles instead of the previous methods (Ahmeda et al., 2020). Biogenic synthesis of nanoparticles from the salts of metal ions is done under 'green' condition, to attain this purpose used reducing factors, an eco-friendly solvent system, and eco-friendly stabilizing (Mahmoudi et al., 2019a,b). Many pharmaceutical plants and microorganisms can be used for formulating nanoparticles, the reduction process of metal ions due to special factors found in organisms that an important principle in the biogenesis of nanoparticles. Furthermore, by removing the environmental impact of biological synthesis, it enables the production of a large number of nanoparticles, which are suitable in morphology and size (Bardania et al., 2020). Since the decade from 1900 to 1909, the application of plant extracts for the reduction of metal ions has been a known method. Due to the lack of understanding of reducing factors in the last 30 years, the interest in researching them has increased (Fahimmunisha et al., 2020). Studies have recently reported that pharmaceutics plants green synthesized metal nanoparticles have efficient anti-cancer features. Metallic nanoparticles have received special attention in the field of medicine. Recently some investigations have shown that some nanoparticles have remedial features and are an excellent alternative to some drugs such as antibacterial, antibacterial, etc (Darvishi et al., 2019).

In recent years, zinc oxide is known as an important compound because of its properties. ZnO is recognized as a multifunctional, fundamental, and non-toxic inorganic material that possesses many applications in different fields (Bayrami et al., 2019a,b). The biosynthetic zinc oxide nanoparticles (ZnONPs) have exhibited considerable potentials as antioxidative, antimicrobial, and anti-cancerous agents (Darvishi et al., 2019). Recent studies have indicated that medicinal plants increase the anti-cancer effects of ZnONPs in the biological synthesizes.

Alhagi maurorum is an herb with many pharmaceutical properties. It belongs to the *Plantae* kingdom, *Fabales*order, *Fabaceae* family, and *Alhagi* genus. Since ancient times people have used *Alhagi maurorum* to cure many diseases related to the respiratory, liver, cardiovascular, gastrointestinal, immune, and urinary and genital systems (Awaad Amani et al., 2006; Hassanshahian et al., 2020; Laghari et al., 2011). The several parts of *Alhagi maurorum* and its products have been used in different world regions for treating diseases such as several cancers, dropsy, rheumatism, asthma, bronchitis, loss of appetite, amenorrhoea, dysmenorrhoea, diarrhea, indigestion, skin eruptions, and worms (Atta and Mouneir, 2004; Almeida et al., 2001). Chemical antioxidant composition that isolated from *Alhagi maurorum* are as fallow: Nonacosane, actinidiolide, 6,10,14-trimethyl-2-pentadecanone, *trans*-β-ionone, pentacosane, 2-nonadecanone, 4-hexyl-2,5-dihydro-2,5-dioxo-3-furanacetic acid, 9-octylheptadecane, drimenol, squalene, tetracosane, docosane, eicosane, octadecane, and drimenol (Abu-Dahab and Afifi, 2007). The therapeutic features of this plant due to its chemical antioxidant composition were mentioned above.

Based on our knowledge, comparative research on anti-osteosarcoma properties of $Zn(NO_3)_2{\cdot}6H_2O$, *Alhagi maurorum* leaf aqueous extract, and ZnONPs synthesized by *Alhagi maurorum* leaf aqueous extract against osteosarcoma cell lines in cellular models has not been done so far. The purpose of this study was to determine the structures of $Zn(NO_3)_2{\cdot}6H_2O$, *Alhagi maurorum* leaf, and ZnONPs against osteosarcoma (G-292, clone A141B1, MG-63, HOS, Hs 707(A).T, and Saos-2) cell lines.

2. Material and methods

2.1. Material

Bovine serum, antimycotic antibiotic solution, 2,2-diphenyl-1-pikrilhydrazil (DPPH), dimethyl sulfoxide (DMSO), decamplmaneh fetal, 4-(Dimethylamino) benzaldehyde, hydrolyzate, Ehrlich solution, and borax-sulfuric acid mixture, Dulbazolic mixture Modified Eagle Medium (DMED), all were purchased from the US Sigma-Aldrich company.

2.2. Preparation and synthesis of ZnO NPs

To produce a green synthesis of ZnONPs first stage is Extraction from *Alhagi maurorum*. The method that we used for achieving this purpose was extracted *Alhagi maurorum* leaf with distilled water in the microwave.

In the recent study, the biosynthesis of ZnONPs was carried out according to the previous studies with some modifications (Laghari et al., 2012; Atta and El-Sooud, 2004). First, 0.4 g of the dried extract was dissolved in 50 mL of deionized water and then was added to 15 mL of $Zn(NO_3)_2{\cdot}6H_2O$ (0.04 M). The pH was adjusted at the pH of 8. Then the flask was placed in an ultrasonic bath for 1 h at 60 °C. The precipitate was formed during the reaction time. The precipitate was washed with ethanol: water (1:1) and then, centrifuged at 12,000 rps. For 15 min and subsequently dried in an oven at 50 °C. The obtained cream powder was kept in a vial for the chemical characterization and evaluation of its biological activity.

2.3. Chemical characterization techniques

To characterize and measure different parameters of the biosynthesized ZnONPs, various techniques, including Ultraviolet–visible (UV–Vis) and Fourier-transform infrared (FTIR) spectroscopy, X-ray diffraction (XRD), scanning electron microscopy (SEM), and Energy Dispersive X-ray Spectrometry (EDS) techniques, were applied. The UV–Vis. spectra were obtained using Photonix Ar 2015 UV–Vis. spectrophotometer (200–800 nm); The FT-IR spectra were recorded using a Shimadzu FT-IR 8400 in the range of 400–4000 cm^{-1} (KBr disc); MIRA3TESCAN-XMU was used to report the FE-SEM Images and EDS result. The XRD pattern of ZnONPs was recorded in the 2θ range of 20–80° by a GNR EXPLORER instrument (voltage of 40 kV, a current of 30 mA, and Cu-Kα radiation 1.5406 Å).

2.4. Antioxidant activities of ZnONPscontaining Alhagi maurorum leaf aqueous extract

Antioxidant activities of ZnONPs, $Zn(NO_3)_2{\cdot}6H_2O$, and *Alhagi maurorum* aqueous extract were evaluated by using 2,2-diphenyl-1-picrylhydrazyl (DPPH) (Shaneza'Aman et al., 2018). First of all 100 mL of CH_3OH was added to the 39.4 g of DPPH, while different concentrations of ZnONPs, $Zn(NO_3)_2{\cdot}6H_2O$, and *Alhagi maurorum* aqueous extract(0–1000 μg/mL) were prepared. Then we added the DPPH solution to the samples that were explained above and incubated at 37 °C for 30 mint. After incubation, the absorbances of the blend were determined at 570 nm. In this experiment, CH_3OH (50%) and butylated hydroxytoluene (BHT) were considered negative and positive controls. The antioxidant activities of the samples were calculated according to the following formula:

$$\text{Inhibition}\,(\%) = \frac{\text{Sample A.}}{\text{Control} - \text{A.}}\,x100$$

All experiments were performed five times.

2.5. Anti-human osteosarcoma properties of ZnONPs containing Alhagi maurorum leaf aqueous extract

In this research, we used the following cell lines to evaluating anti-human osteosarcoma and cytotoxicity effects of ZnONPs, $Zn(NO_3)_2{\cdot}6H_2O$, and *Alhagi maurorum* using an 3-(4,5-dime thylthiazol-2-yl)-2,5-diphenyl-2H-tetrazolium bromide (MTT) method.

(a) Human osteosarcoma cell lines:
- G-292, clone A141B1
- MG-63
- HOS
- Hs 707(A).T
- Saos-2

(b) Normal cell line:
- Human umbilical vein endothelial cells (HUVECs).

They were then cultured as a monolayer culture in 90% RPMI-1640 medium and 10% fetal serum and supplemented with 200 mg/mL streptomycin, 125 mg/mL penicillin, and 8 mg/mL amphotericin B. The culture was then exposed to 0.5 atmospheric carbon dioxide at 37 °C, on which the tests were performed after at least ten successful passages. MTT assay a method used to investigate the toxic effects of various materials on various cell lines, including non-cancer and cancer cells. To evaluate the cell toxicity effects of the compounds used in this research, the cells were transferred from the T25 flask to the 96-well flasks. In each cell of the 96-cell flasks, 7000 cells of cancer and fibroblast cell lines were cultured, and the volume of each cell was eventually increased to 100 μL. Before treating the cells in the 96-well flak, the density of cells was increased to 70%, so the 96-well flasks were incubated for 24 h to obtain the cell density of 7×10^3. Next, the initial culture medium was discarded, and variable concentrations (0–1000 μg/mL) of ZnONPs, $Zn(NO_3)_2{\cdot}6H_2O$, and *Alhagi maurorum* were incubated at 37 °C and 0.5 CO_2 for 24, 48, and 72 h. Then, 20 μL MTT was added to each well after a certain amount of time. Next, 100 μL DMSO solvent was added to each well. They were then kept at room temperature for 25 min and read at 570 nm by a microtitre plate reader (Arunachalam et al., 2013).

The cell lines were treated with the hydroalcoholic extract (1.25 mg/mL), which inhibited about 20% of the cell growth. Annexin/PI method was used to determine the apoptosis level in the treated and control cell lines using a flow cytometry machine. To the experiment, the cell lines were treated with a variable concentrations (0–1000 μg/mL) of ZnONPs, Zn $(NO_3)_2{\cdot}6H_2O$, and *Alhagi maurorum* for 24 h. Cells were irrigated with phosphate-buffered saline (PBS). After centrifugation, buffer binding was added to the obtained precipitate. Then, 5 μL Annexin V dye was added and incubated for 15 min at 25 °C. Cells were washed with the binding solution, following which 10 μL PI dye was added. Finally, cell analysis was done by a flow cytometry machine according to the below formula (Arunachalam et al., 2013):

$$\text{Cell viability } (\%) = \frac{\text{Sample A.}}{\text{Control A.}} \times 100$$

All experiments were performed five times.

2.6. Statistical analysis

The data were gathered and given into the "SPSS-24" a computer software program and was analyzed by "one-way ANOVA", and then Duncan posthoc test ($p \leq 0.01$).

3. Results and discussion

In this experiment, we formulated ZnONPs by using of *Alhagi maurorum* leaf aqueous extract. Furthermore, in vitro condition, we evaluated the anti-human osteosarcoma activities of ZnONPs, $Zn(NO_3)_2{\cdot}6H_2O$, and *Alhagi maurorum* (0–1000 μg/mL) against common human osteosarcoma cell lines i.e.G-292, clone A141B1, MG-63, HOS, Hs 707(A).T, and Saos-2.

3.1. Characterization of ZnONPs

3.1.1. UV–visible spectroscopy analysis

Fig. 1 presents the UV–Vis. spectrum of biosynthesized ZnONPs using *Alhagi maurorum* extract. The result of UV–Vis. spectroscopy confirms the formation of ZnONPs. The peaks at 271 and 386 nm belong to the biosynthetic ZnONPs. This observation is in good agreement with the previous studies on biosynthesized of ZnONPs nanoparticles (Sharmila et al., 2019).

3.1.2. FT-IR analysis

In the FT-IR spectra of metal oxides, the vibration band for metal–oxygen bond usually appears in 400–700 cm^{-1}. Fig. 2 exhibits the spectra of ZnONPs. The peaks at 443 and 503 cm^{-1} attribute to the bending vibration of Zn-O. These peaks for iron oxide nanoparticles have been reported previously with a small difference in the wavenumber (Sharmila et al., 2019; Dobrucka et al., 2018). FT-IR technique is a reliable method to evaluate the secondary plant metabolites as the capping and reducing agents of ferric chloride precursor to ZnONPs. FT-IR spectra of ZnONPs and *Alhagi maurorum* extract are very similar to each other; this similarity can approve the biosynthesis of the iron oxide nanoparticles. The presences of different-IR bands correlate to the presence of various functional groups in *Alhagi maurorum* extract. for instance, Peaks in 3427 and 2923 cm^{-1} related to O—H and aliphatic C—H stretching; the peaks at a range of 1548 and 1743 cm^{-1} correspond to C═C and C═O stretching, and peaks at 1151 and 1078 cm^{-1} could be ascribed to —C—O and —C—O—C stretching These peaks can be considered for the presence of various compounds in the plant extract such as phenolic, flavonoid, triterpenes which have been reported previously (Akbar, 2020; Behbahani, 2014).

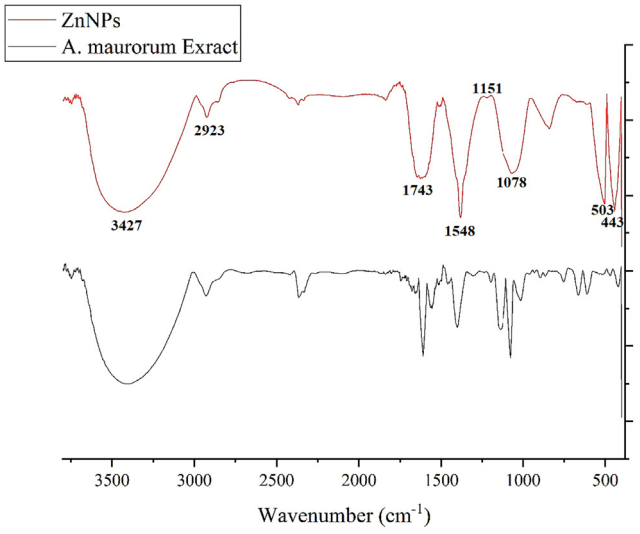

Fig. 2 FT-IR Spectra of Alhagi maurorum extract and ZnONPs.

3.1.3. XRD analysis

Fig. 3 shows the XRD pattern of ZnONPs. The result, same to FT-IR spectra, approves the synthesis of zinc oxide. The peaks at 31.78, 34.38, 36.36, 47.48, 56.50, 62.78, and 67.81 corresponding to ZnONPs (1 0 0), (0 0 2), (1 0 1), (1 0 2), (1 1 0), (1 0 3), and (1 1 2) planes. These peaks are matched and those

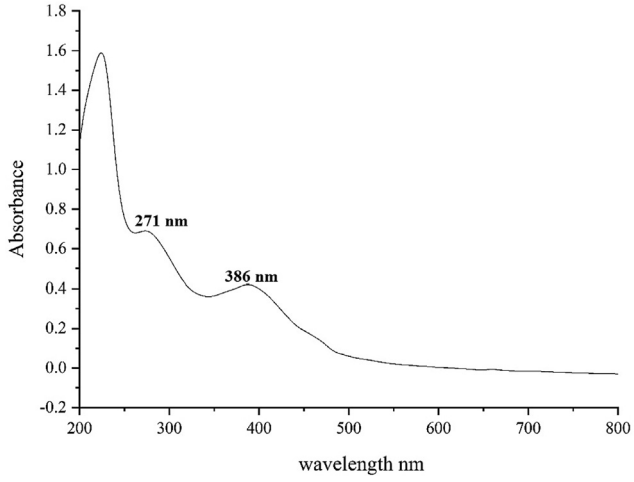

Fig. 1 UV–Vis. spectra of biosynthesized ZnO.

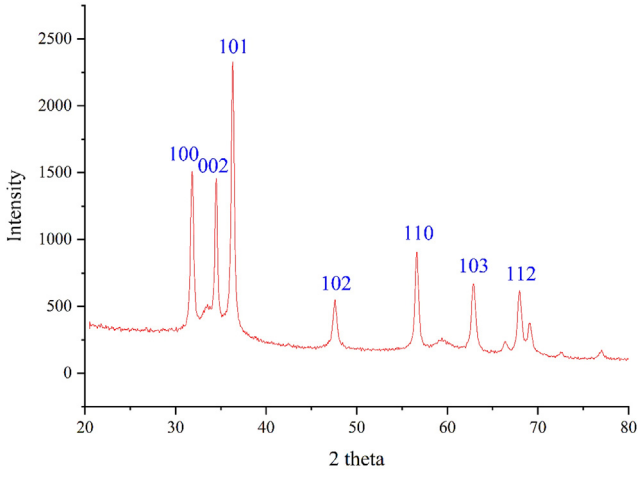

Fig. 3 XRD Pattern of ZnONPs.

of zinc oxide obtained from standard database ICDD PDF card no. 01-080-3002. The crystallinity of the ZnONPs has been accepted using the XRD diffractogram. The peaks at different degrees are also reported previously. The average crystal size of ZnONPs was calculated using X-ray diffraction according to Scherrer equation

$$D = \frac{k\lambda}{\beta\cos\theta}$$

The ZnO nanoparticles had an average crystal size of 21.46 nm. A few previous studies have reported various crystalline sizes according to XRD analysis for the biosynthesized ZnONPs using plant extracts. The reported size was in the range of 16.7–59 nm (Ezealisiji et al., 2019; Bayrami et al., 2018).

3.1.4. SEM analysis

FE-SEM images of ZnONPs is shown in Fig. 4(a–b). The images depict a spherical morphology for the ZnONPs. This morphology for biosynthesized ZnONPs has been reported previously (Arvanag et al., 2019). The figure also confirms the uniformity, well dispersed, and homogeneous of the ZnONPs. Like the other metallic nanoparticles, which have synthesized using green chemistry approaches, a propensity to aggregate is observed for ZnONPs. This property has been reported by others for ZnONPs, CdNPs, CuNPs, AgNPs, and TiNPs (Harshiny et al., 2015; Rao and Pennathur, 2017). The diameter of particle size for ZnONPs was on average of 27.92 nm. Our review of literature 10–35.62 nm were reported for biosynthesized of zinc oxide using plant extracts as the capping agent for NPs (Ghidan et al., 2016; Baghayeri et al., 2018; Seydi et al., 2019).

3.1.5. EDS analysis

The EDS analysis of the synthesized, as a semi-quantitative technique to recognize the elements, is shown in Fig. 5. The diagram presents the elemental composition profile of the ZnONPs. The presence of zinc was confirmed by the signals around 1 keV (for ZnLα), below 9 keV (ZnKα), and below 10 keV (for ZnKβ). These signals are as well as match to those of biosynthesized ZnONPs that reported previously (Mahdavi et al., 2019a,b; Saha et al., 2018). A single after 0.5 keV belongs to oxygen. This signal can be attributed to the oxygen in zinc oxide nanoparticles and to the organic molecules present in *Alhagi maurorum* extract that linked to the surface of ZnONPs. The presence of carbon on the surface of ZnONPs was confirmed by the signal before 0.3 Kev.

3.2. Cytotoxicity and anti-human osteosarcoma activities of ZnONPscontaining Alhagi maurorum leaf aqueous extract

In this study, the treated cells with different concentrations of the present ZnONPs, $Zn(NO_3)_2{\cdot}6H_2O$, and *Alhagi maurorum* leaf aqueous extract were assessed by MTT assay for 24, 48, and 72 about the cytotoxicity properties on normal (HUVEC) and bone malignancy cell lines i.e. G-292, clone A141B1, MG-63, HOS, Hs 707(A).T, and Saos-2. The absorbance rate was evaluated at 570 nm, which represented viability on normal cell line (HUVEC) even up to 1000 μg/mL for ZnONPs, $Zn(NO_3)_2{\cdot}6H_2O$, and *Alhagi maurorum* leaf aqueous extract (Tables 1 and 2). The viability of malignant bone cell line reduced dose-dependently in the presence of ZnONPs, $Zn(NO_3)_2{\cdot}6H_2O$, and *Alhagi maurorum* leaf aqueous extract. The IC50 of ZnONPs were 234 ± 0, 285 ± 0, 327 ± 0, 372 ± 0, and 341 ± 0 μg/mL against HOS, MG-63, G-292, clone A141B1, Saos-2, and Hs 707(A).Tcell lines, respectively.

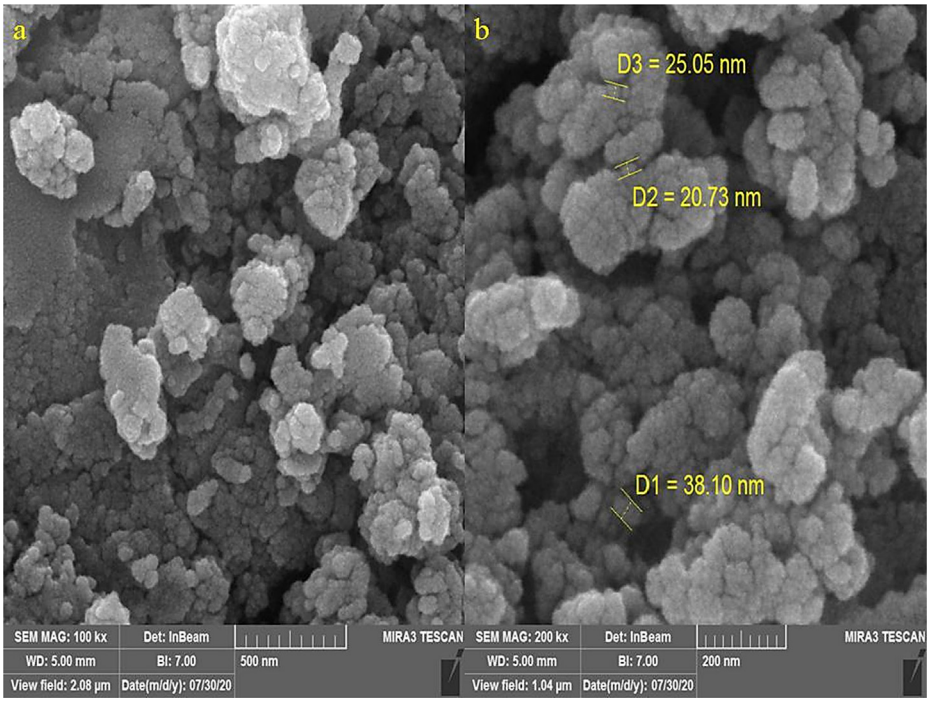

Fig. 4 SEM Images of ZnONPs.

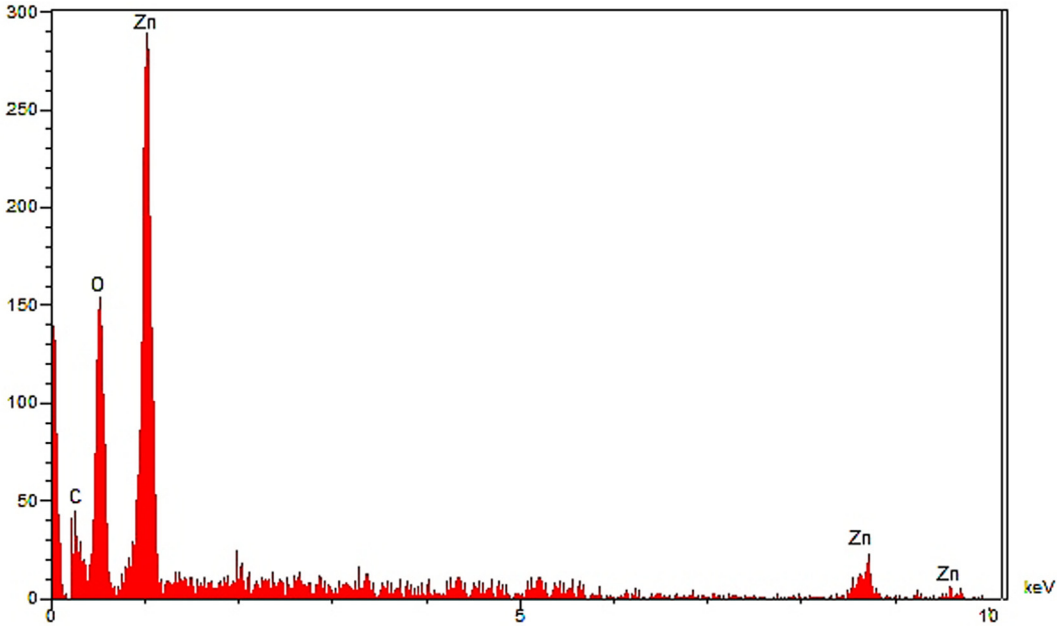

Fig. 5 EDS analysis of ZnONPs.

While, the IC50 of *Alhagi maurorum* leaf aqueous extract were 419 ± 0, 468 ± 0, 532 ± 0, 550 ± 0, and 516 ± 0 μg/mL against HOS, MG-63, G-292, clone A141B1, Saos-2, and Hs 707(A).T cell lines, respectively.

Zinc nanoparticles have various parameters such as shape, size, texture, etc. Sizes have very significant properties in the therapeutic effects of nanoparticles, some studies reported that small zinc nanoparticles have better entrance into cells and have significant anti-cancer activities (Pai et al., 2019; Tahvilian et al., 2019). It has been assessed that particle size lower than 50 nm showed an excellent remedial feature in the corresponding cancer cell lines (Mao et al., 2016; Namvar et al., 2014; Sankar et al., 2014). As you see in Fig. 4 of our study, the average size of ZnONPs synthesized by *Alhagi maurorum* seed aqueous extract is less than 50 nm. Zinc nanoparticles have been utilized to treat various cancers including Lewis lung carcinoma, human glioma, human lung cancer, uterus cancer, lung epithelial cancer, colon cancer, and mammary carcinoma (Katata-Seru et al., 2018; Sangami and Manu, 2017).

ZnO NPs present certain cytotoxicity in cancer cells mainly by themselves based on a higher intracellular release of dissolved zinc ions, followed by increased ROS induction and induced cancer cell death via the apoptosis signaling pathway. Sharma et al. explored the effects of ZnO NPs on human liver cancer HepG2 cells and its possible pharmacological mechanism. ZnO NPs-exposed HepG2 cells presented higher cytotoxicity and genotoxicity, which were associated with cell apoptosis mediated by the ROS triggered mitochondrial pathway. The loss of the mitochondrial membrane potential could open outer membrane pores resulting in the release of some related apoptotic proteins including cytochrome *c* into the cytosol and activate the caspase. Mechanistic studies had proved that the loss of mitochondrial membrane potential-mediated HepG2 cell apoptosis was mainly due to the decrease in mitochondrial membrane potential and Bcl-2/Bax ratios accompanying with the activation of caspase-9. Besides, ZnO NPs could noticeably activate p38 and JNK and induce and attract $p53^{ser15}$ phosphorylation but was not dependent on JNK and p38 pathways. These results afforded valuable insights into the mechanism of ZnO NPs-induced apoptosis in human liver HepG2 cells (Beheshtkhoo et al., 2018; Oganesvan et al., 1991; Radini et al., 2018). Moghaddam et al. biosynthesized ZnO NPs using a new strain of yeast (*Pichia kudriavzevii* GY1) and evaluated their anticancer activity in breast cancer MCF-7 cells. ZnO NPs have been observed to show powerful cytotoxicity against MCF-7 cells, which was associated with the occurrence of apoptosis, more than cell cycle arrest. The ZnO NPs-induced apoptosis was mainly through both extrinsic and intrinsic apoptotic pathways, and some antiapoptotic genes of Bcl-2, AKT1, and JERK/2 were downregulated, while pro-apoptotic genes of p21, p53, JNK, and Bax were upregulated. ZnO NPs have been widely used in cancer therapy and reported to induce a selective cytotoxic effect on cancer cell proliferation (Sharma et al., 2012; Boroumand Moghaddam et al., 2017). Chandrasekaran and Pandurangan investigated the cytotoxicity of ZnO nanoparticles against cocultured C2C12 myoblastoma cancer cells and 3T3-L1 adipocytes, which showed that ZnO NPs could be more cytotoxic to C2C12 myoblastoma cancer cells than 3T3-L1 cells. Compared to 3T3-L1 cells, it appeared that ZnO NPs inhibited C2C12 cell proliferation and caused marked apoptosis via a ROS-mediated mitochondrial intrinsic apoptotic pathway and p53, Bax/Bcl-2 ratio, and caspase-3 pathways (Chandrasekaran and Pandurangan, 2016). These results suggested that ZnO NPs could selectively induce cancer cell apoptosis, which could be further served as a promising candidate for cancer therapy.

As be seen in the above tables, the best results of cytotoxicity and anti-human osteosarcoma properties of ZnONPs and

Table 1 The anti-osteosarcoma properties of $Zn(NO_3)_2$, *Alhagi maurorum* leaf aqueous extract, and ZnONPs against human osteosarcoma cell line.

Concentration (μg/ml)	Cell Viability (%)					
	HUVEC	G-292, clone A141B1	MG-63	HOS	Hs 707(A).T	Saos-2
$Zn(NO_3)_2$ (0)	100 ± 0^{a}	100 ± 0^{a}	100 ± 0^{a}	100 ± 0^{a}	100 ± 0^{a}	100 ± 0^{a}
$Zn(NO_3)_2$ (1)	100 ± 0^{a}	100 ± 0^{a}	100 ± 0^{a}	99.4 ± 0.89^{a}	100 ± 0^{a}	99.9^{a}
$Zn(NO_3)_2$ (2)	99.6 ± 0.89^{a}	99.8 ± 1.09^{a}	99.8 ± 1.09^{a}	99.2 ± 0.83^{a}	100 ± 0^{a}	99.4^{a}
$Zn(NO_3)_2$ (3)	99 ± 1^{a}	99.6 ± 1.14^{a}	99.4 ± 0.89^{a}	99 ± 0.7^{a}	99 ± 0.7^{a}	98 ± 1.22^{a}
$Zn(NO_3)_2$ (7)	97.4 ± 0.54^{a}	99 ± 0.7^{a}	98.6 ± 0.89^{a}	97 ± 1.22^{a}	98.8 ± 1.09^{a}	97.4 ± 0.89^{a}
$Zn(NO_3)_2$ (15)	95.4 ± 0.54^{a}	98 ± 1^{a}	97.2 ± 1.3^{a}	95.6 ± 1.14^{a}	97.4 ± 0.54^{a}	96 ± 0.7^{a}
$Zn(NO_3)_2$ (31)	92.6 ± 0.89^{a}	97.4 ± 0.89^{a}	95.8 ± 1.09^{a}	92 ± 1^{a}	96.6 ± 0.89^{a}	94 ± 1^{a}
$Zn(NO_3)_2$ (62)	86.4 ± 0.89^{ab}	95 ± 0.7^{a}	92.2 ± 0.83^{a}	88.4 ± 0.54^{ab}	94.2 ± 1.3^{a}	90 ± 1.22^{a}
$Zn(NO_3)_2$ (125)	80 ± 0.7^{ab}	92.2 ± 0.83^{a}	87.2 ± 0.83^{ab}	83.8 ± 1.09^{ab}	91.2 ± 0.83^{a}	85.6 ± 0.89^{ab}
$Zn(NO_3)_2$ (250)	73 ± 1.22^{b}	87.6 ± 1.14^{ab}	81.2 ± 1.3^{ab}	76 ± 1.22^{ab}	85.6 ± 0.89^{ab}	79.6 ± 0.89^{ab}
$Zn(NO_3)_2$ (500)	63.2 ± 0.83^{b}	80.6 ± 0.89^{ab}	74 ± 1^{b}	69.8 ± 1.09^{b}	77.4 ± 0.54^{ab}	72.4 ± 0.89^{b}
$Zn(NO_3)_2$ (1000)	51 ± 1^{bc}	70 ± 0.7^{b}	65.2 ± 1.3^{b}	60 ± 0.7^{bc}	69.8 ± 1.09^{b}	64.8 ± 1.09^{b}
A. maurorum (0)	100 ± 0^{a}	100 ± 0^{a}	100 ± 0^{a}	100 ± 0^{a}	100 ± 0^{a}	100 ± 0^{a}
A. maurorum (1)	100 ± 0^{a}	99.4 ± 0.89^{a}	99.8 ± 1.09^{a}	99.4 ± 0.89^{a}	99.4 ± 0.89^{a}	99.6 ± 1.14^{a}
A. maurorum (2)	100 ± 0^{a}	99.2 ± 1.3^{a}	99.4 ± 0.89^{a}	99 ± 0.7^{a}	99 ± 1.22^{a}	99.4 ± 0.54^{a}
A. maurorum (3)	99.8 ± 1.09^{a}	98 ± 1.22^{a}	97 ± 1^{a}	97 ± 1^{a}	98.2 ± 0.83^{a}	98.4 ± 0.89^{a}
A. maurorum (7)	99.6 ± 1.14^{a}	96.6 ± 0.89^{a}	95.6 ± 1.14^{a}	95.2 ± 1.3^{a}	96.2 ± 1.3^{a}	97 ± 1.22^{a}
A. maurorum (15)	99.2 ± 0.83^{a}	94.6 ± 1.14^{a}	91.4 ± 0.54^{a}	91.6 ± 1.14^{a}	93.2 ± 0.83^{a}	94.4 ± 0.54^{a}
A. maurorum (31)	98.6 ± 1.14^{a}	91 ± 0.7^{a}	85 ± 1^{ab}	84.6 ± 1.14^{ab}	88.4 ± 0.89^{ab}	90 ± 1^{a}
A. maurorum (62)	98.4 ± 0.89^{a}	84 ± 1.22^{ab}	77.2 ± 1.3^{ab}	76.8 ± 1.09^{ab}	80.6 ± 0.89^{ab}	83.6 ± 0.89^{ab}
A. maurorum (1 2 5)	97.4 ± 0.54^{a}	75 ± 1^{b}	69.2 ± 0.83^{b}	68 ± 1.22^{b}	71.2 ± 0.44^{b}	75 ± 1.22^{b}
A. maurorum (250)	97 ± 0.7^{a}	64.6 ± 0.89^{b}	60.2 ± 0.83^{bc}	58.6 ± 1.14^{bc}	61.8 ± 1.09^{b}	64.2 ± 0.44^{b}
A. maurorum (500)	96.4 ± 0.54^{a}	51.2 ± 0.83^{bc}	48 ± 1^{bc}	46.4 ± 0.89^{bc}	50.2 ± 0.44^{bc}	52 ± 0.7^{bc}
A. maurorum (1000)	95.6 ± 0.89^{a}	33.8 ± 1.09^{c}	33 ± 1.22^{c}	31.8 ± 1.09^{c}	35.8 ± 1.09^{c}	35.8 ± 1.09^{c}
ZnONPs (0)	100 ± 0^{a}	100 ± 0^{a}	100 ± 0^{a}	100 ± 0^{a}	100 ± 0^{a}	100 ± 0^{a}
ZnONPs (1)	100 ± 0^{a}	99.6 ± 1.14^{a}	99.6 ± 0.89^{a}	99.6 ± 0.89^{a}	99 ± 1^{a}	99.6 ± 0.89^{a}
ZnONPs (2)	100 ± 0^{a}	99 ± 0.7^{a}	98.4 ± 0.89^{a}	98.8.2 ± 0.44^{a}	99 ± 0.7^{a}	99 ± 0.7^{a}
ZnONPs (3)	99.6 ± 1.14^{a}	97.4 ± 0.89^{a}	97 ± 1.22^{a}	96.2 ± 1.3^{a}	97.2 ± 0.83^{a}	97.2 ± 0.44^{a}
ZnONPs (7)	99.4 ± 0.54^{a}	95.6 ± 0.89^{a}	94 ± 1^{a}	92.2 ± 0.83^{a}	94.2 ± 0.44^{a}	95 ± 0.7^{a}
ZnONPs (15)	99.2 ± 0.83^{a}	92.2 ± 0.83^{a}	90.2 ± 0.83^{a}	86.7.2 ± 0.44^{ab}	90.2 ± 1.3^{a}	91.2 ± 0.83^{a}
ZnONPs (31)	98.6 ± 0.89^{a}	88.8 ± 1.09^{ab}	83.4 ± 0.89^{ab}	79.2 ± 1.3^{ab}	84.5 ± 0.7^{ab}	86.8 ± 0.7^{ab}
ZnONPs (62)	98.2 ± 0.83^{a}	80.4 ± 0.89^{ab}	75 ± 1.22^{b}	69.2 ± 0.44^{b}	77.2 ± 0.44^{ab}	80.2 ± 0.44^{ab}
ZnONPs (125)	97.6 ± 0.89^{a}	71 ± 1^{b}	64.8 ± 1.09^{b}	58.2 ± 0.44^{bc}	69.4 ± 0.89^{b}	71.8 ± 1.09^{b}
ZnONPs (250)	96 ± 0.7^{a}	56.6 ± 1.14^{bc}	52.6 ± 1.14^{bc}	47 ± 1.22^{bc}	56 ± 1.22^{bc}	58 ± 1^{bc}
ZnONPs (500)	94 ± 1.22^{a}	40 ± 0.7^{c}	37.6 ± 0.89^{c}	30 ± 0.7 ^{cd}	41.2 ± 0.83^{c}	43 ± 1^{c}
ZnONPs (1000)	90.2 ± 1.3^{a}	20.2 ± 0.83 ^{cd}	18.6 ± 1.14^{d}	12.2 ± 0.44^{d}	24 ± 1 ^{cd}	26.6 ± 0.89 ^{cd}

The letters indicate the significant difference between experimented groups ($p \leq 0.01$).

Table 2 The IC50 of $Zn(NO_3)_2$, *Alhagi maurorum* leaf aqueous extract, and ZnONPs in cytotoxicity and anti-osteosarcoma tests.

	$Zn(NO_3)_2$ (μg/mL)	*Alhagi maurorum* (μg/mL)	ZnONPs (μg/mL)
IC50 against HUVEC	–	–	–
IC50 against HOS	–	419 ± 0^{b}	234 ± 0^{d}
IC50 against MG-63	–	468 ± 0^{ab}	285 ± 0 ^{cd}
IC50 against G-292, clone A141B1	–	532 ± 0^{a}	327 ± 0^{c}
IC50 against Saos-2	–	550 ± 0^{a}	372 ± 0^{bc}
IC50 against Hs 707(A).T	–	516 ± 0^{a}	341 ± 0^{c}

The letters indicate the significant difference between experimented groups ($p \leq 0.01$).

Alhagi maurorum leaf aqueous extract are in the case of HOS without any cytotoxicity against normal cell line, i.e. HUVEC.

3.3. Antioxidant features of ZnONPs containing Alhagi maurorum leaf aqueous extract

In this study, we assessed the antioxidant properties of *Alhagi maurorum* leaf aqueous extract green-synthesized zinc nanoparticles by using the DPPH test. DPPH test is used to evaluate the free radical scavenging activities of different antioxidant materials. This approach depends on the reduction of free radical DPPH by antioxidants in the absence of other free radicals, this action generates a color that absorption intensity can be evaluated by spectroscopy. The highest light absorption of DPPH radical at 515–520 nm in which methanolic solution is purple and acts as an electron absorber of a

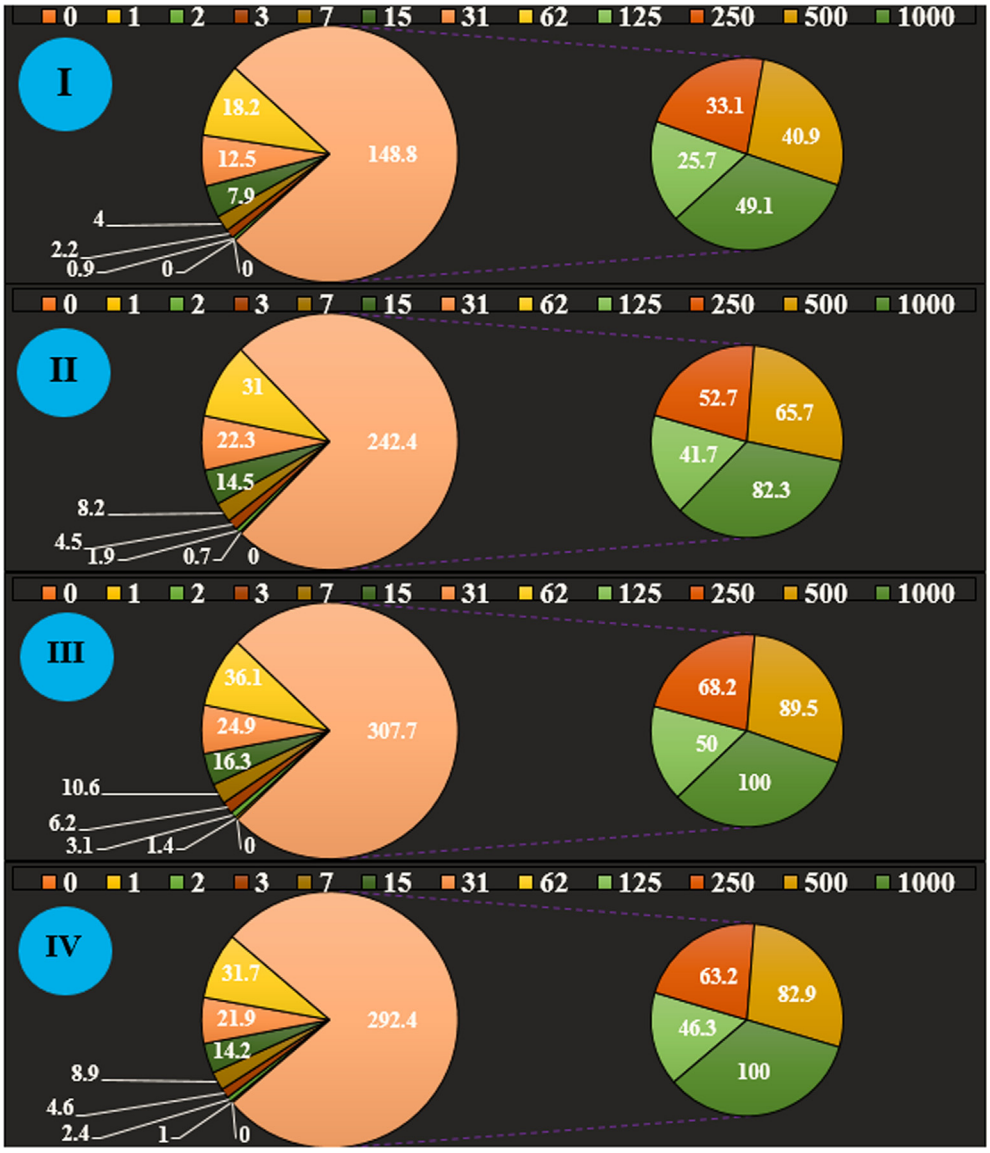

Fig. 6 The antioxidant properties of $Zn(NO_3)_2$ (I), *Alhagi maurorum* leaf aqueous extract (II), ZnONPs (III), and BHT (IV) against DPPH.

Table 3 The IC50 of $Zn(NO_3)_2$, *Alhagi maurorum* leaf aqueous extract, ZnONPs, and BHT in the antioxidant test.

	$Zn(NO_3)_2$ (μg/mL)	*Alhagi maurorum* (μg/mL)	ZnONPs (μg/mL)	BHT (μg/mL)
IC50 against DPPH	–	221 ± 0^{c}	125 ± 0^{a}	149 ± 0^{b}

The letters indicate the significant difference between experimented groups ($p \leq 0.01$).

donor molecule like an antioxidant, thus changing DPPH to DPPH2. Consequently, the purple color of the solution becomes yellow, therefore the absorption intensity decreases at 515–520 nm. We can find out the importance of antioxidant activities by evaluating the absorption intensity reduction through spectroscopy. The scavenging capacity of *Alhagi maurorum* leaf aqueous extract green-synthesized zinc nanoparticles and BHT at different concentrations expressed as percentage inhibition has been indicated in Fig. 6.

In the antioxidant test, the IC50 of *Alhagi maurorum* leaf aqueous extract, ZnONPs, and BHT were 144 and 201 μg/mL, respectively (Table 3).

Studies have shown that the antioxidant features of ZnONPs green synthesized by pharmaceutical herbs are more significant than other metal nanoparticles. So far considerable antioxidant activities of metallic nanoparticles green-synthesized by several pharmaceutics herbs like *Gundeliatourne fortii* L., *Allium noeanum* Reut. ex Regel, *Falcaria vulgaris*,

Thymus vulgaris, and *Camellia sinensis* have been confirmed. ZnONPs green-synthesized by pharmaceutics herbs shows noticeable antioxidant activities against free radicals formation in the living system. The ZnONPs green-synthesized-formulated have important redox activities and have a noticeable role in free radicals dismantle. Mahdavi et al. indicated the zinc nanoparticles green-synthesized by *Ziziphora clinopodioides* Lam leaves aqueous extract had excellent antioxidant effects against DPPH free radicals. In the previous study, DPPH free radical scavenging effect of *Ziziphora clinopodioides* and ZnONPs@Ziziphora revealed strong inhibition similar to BHT. The IC50 of BHT, *Ziziphora clinopodioides*, and ZnONPs@Ziziphora were 378, 378, and 250 μg/ml, respectively (Mahdavi et al., 2019a,b).

Forgoing researches have revealed that phenolic and flavonoids compounds appended to the metallic nanoparticles have important antioxidant activities. As mentioned in the introduction *Alhagi maurorum* contains antioxidant compounds Nonacosane, actinidiolide, 6,10,14-trimethyl-2-pentadecanone, *trans*-β-ionone, pentacosane, 2-nonadecanone, 4-hexyl-2,5-di hydro-2,5-dioxo-3-furanacetic acid, 9-octylheptadecane, drimenol, squalene, tetracosane, docosane, eicosane, octadecane, and drimenol.

Maybe important anti-human osteosarcoma potentials of ZnONPs synthesized by *Alhagi maurorum* leaf aqueous extract against malignant bone cell lines i.e., HOS, MG-63, G-292, clone A141B1, Saos-2, and Hs 707(A).T due to their antioxidant activities. Corresponding reports have indicated the antioxidant materials like pharmaceutics plants and metallic nanoparticles especially zinc nanoparticles reduce the volume of tumors by scavenging free radicals (Katata-Seru et al., 2018). Generally, the presence of free radicals in the body causes countless chain reactions in the body that gives rise to the production of more free radicals, also causes a variety of mutations in the structure of DNA and RNA, and cause an uncontrolled increase in malignant cell proliferation and finally damage the body (Sangami and Manu, 2017; Beheshtkhoo et al., 2018). The high concentration of free radicals present in all kinds of cancer, free radicals causes tumorigenesis and angiogenesis (Sangami and Manu, 2017). Many studies worldwide reported that zinc nanoparticles synthesized by pharmaceutics plants have a significant role in eliminating free radicals and are involved in preventing the growth of malignant cells (Oganesvan et al., 1991; Radini et al., 2018).

4. Conclusion

In this research, the zinc nanoparticles were attained from the reaction between $Zn(NO_3)_2{\cdot}6H_2O$ and *Alhagi maurorum* leaf aqueous extract in vitro condition. EDS, XRD, SEM, UV–Vis, and FT-IR methods were utilized to evaluate nanoparticle characteristics. The results of these techniques revealed that zinc nanoparticles had been synthesized in the best way. Base on the FT-IR spectrum the presence of a significant number of antioxidant compounds produced appropriate conditions for the reduction of zinc. According to the XRD analysis, 21.46 was measured for ZnONPs crystal size. SEM images exhibited a uniform spherical morphology in size of 27.92 nm for the biosynthesized nanoparticles respectively. The zinc nanoparticles showed the best antioxidant activities against DPPH. ZnONPs had appropriate anti-human osteosarcoma activities dose-dependently against HOS, MG-63, G-292, clone A141B1, Saos-2, and Hs 707(A)cell lines without any cytotoxicity on the normal cell line (HUVEC). The IC50 of ZnONPs were 234 ± 0, 285 ± 0, 327 ± 0, 372 ± 0, and 341 ± 0 μg/mL against HOS, MG-63, G-292, clone A141B1, Saos-2, and Hs 707(A).T cell lines, respectively. After clinical study zinc nanoparticles containing *Alhagi maurorum* leaf aqueous extract can be utilized as an efficient drug in treating bone cancer in humans.

Declaration of Competing Interest

The authors declare that they have no known competing financial interests or personal relationships that could have appeared to influence the work reported in this paper.

Acknowledgment

This project was supported by Researchers Supporting Project number (RSP-2020/230) King Saud University, Riyadh, Saudi Arabia.

References

Boroumand Moghaddam, A., Moniri, M., Azizi, S., Abdul Rahim, R., Bin Ariff, A., Navaderi, M., Mohamad, R., 2017. Eco-friendly formulated zinc oxide nanoparticles: induction of cell cycle arrest and apoptosis in the MCF-7 cancer cell line. Genes 8 (10), 281. https://doi.org/10.3390/genes8100281.

Abu-Dahab, R., Afifi, F., 2007. Antiproliferative activity of selected medicinal plants of Jordan against a breast adenocarcinoma cell line (MCF7). Sci. Pharm. 75 (3), 121–146.

Ahmeda, A., Zangeneh, A., Zangeneh, M.M., 2020. Green synthesis and chemical characterization of gold nanoparticle synthesized using Camellia sinensis leaf aqueous extract for the treatment of acute myeloid leukemia in comparison to daunorubicin in a leukemic mouse model. Appl. Organometal. Chem. 34 (3). https://doi.org/10.1002/aoc.v34.310.1002/aoc.5290.

Akbar, S., 2020. Handbook of 200 Medicinal Plants: A Comprehensive Review of Their Traditional Medical Uses and Scientific Justifications. Springer Nature.

Almeida, R., Navarro, D., Barbosa-Filho, J., 2001. Plants with central analgesic activity. Phytomedicine 8 (4), 310–322.

Arunachalam, K.D., Annamalai, S.K., Hari, S., 2013. One-step green synthesis and characterization of leaf extract-mediated biocompatible silver and gold nanoparticles from Memecylon umbellatum. Int. J. Nanomed. 8, 1307.

Arvanag, F.M., Bayrami, A., Habibi-Yangjeh, A., Rahim Pouran, S., 2019. A comprehensive study on antidiabetic and antibacterial activities of ZnO nanoparticles biosynthesized using Silybum marianum L seed extract. Mater. Sci. Eng., C 97, 397–405.

Atta, A.H., EL-Sooud, K.A., 2004. The antinociceptive effect of some Egyptian medicinal plant extracts. J. Ethnopharmacol. 95 (2-3), 235–238.

Atta, A.H., Mouneir, S.M., 2004. Antidiarrhoeal activity of some Egyptian medicinal plant extracts. J. Ethnopharmacol. 92 (2-3), 303–309.

Awaad Amani, A.S., Maitland, D.J., Soliman, G.A., 2006. Antiulcerogenic Activity of Alhagi maurorum. Pharm. Biol. 44 (4), 292–296.

Mahdavi, B., Paydarfard, S., Zangeneh, M.M., Goorani, S., Seydi, N., Zangeneh, A., 2019a. Appl. Organometal. Chem. 33, e5248.

Baghayeri, M., Mahdavi, B., Hosseinpor-Mohsen Abadi, Z., Farhadi, S., 2018. Green synthesis of silver nanoparticles using water extract of Salvia leriifolia: antibacterial studies and applications as

catalysts in the electrochemical detection of nitrite. Appl. Organomet. Chem. 32 (2). https://doi.org/10.1002/aoc.v32.210.1002/aoc.4057.

Bardania, Hassan, Mahmoudi, Reza, Bagheri, Hamed, Salehpour, Zeinab, Fouani, Mohamad Hassan, Darabian, Bita, Khoramrooz, Seyed Sajjad, Mousavizadeh, Ali, Kowsari, Majid, Moosavifard, Seyyed, Javeshghani, Danesh, Alipour, Mohsen, Akrami, Mohammad, 2020. Facile preparation of a novel biogenic silver-loaded Nanofilm with intrinsic anti-bacterial and oxidant scavenging activities for wound healing. Sci. Rep. 10 (1), 6129.

Bayrami, A., Alioghli, S., Rahim Pouran, S., Habibi-Yangjeh, A., Khataee, A., Ramesh, S., 2019a. A facile Ultrasonic-aided biosynthesis of ZnO nanoparticles using *Vaccinium arctostaphylos* L. leaf extract and its antidiabetic, antibacterial, and oxidative activity evaluation. Ultrason. Sonochem. 55, 57–66.

Bayrami, A., Ghorbani, E., Rahim Pouran, S., Habibi-Yangjeh, A., Khataee, A., Bayrami, M., 2019b. Enriched zinc oxide nanoparticles by Nasturtium officinale leaf extract: Joint ultrasound-microwave-facilitated synthesis, characterization, and implementation for diabetes control and bacterial inhibition. Ultrason. Sonochem. 58, 104613. https://doi.org/10.1016/j.ultsonch.2019.104613.

Bayrami, A., Parvinroo, S., Habibi-Yangjeh, A., Rahim Pouran, S., 2018. Bio-extract-mediated ZnO nanoparticles: microwave-assisted synthesis, characterization and antidiabetic activity evaluation. Artif. Cells Nanomed. Biotechnol. 46 (4), 730–739.

Behbahani, M., 2014. Evaluation of in vitro anticancer activity of Ocimum basilicum, Alhagi maurorum, Calendula officinalis and their parasite Cuscuta campestris. PloS One 9 (12).

Beheshtkhoo, N., Kouhbanani, M.A.J., Savardashtaki, A., Amani, A. M., Taghizadeh, S., 2018. Green synthesis of iron oxide nanoparticles by aqueous leaf extract of Daphne mezereum as a novel dye removing material. Appl. Phys. A 124 (5), 363.

Darvishi, E., Kahrizi, D., Arkan, E., 2019. Comparison of different properties of zinc oxide nanoparticles synthesized by the green (using Juglans regia L. leaf extract) and chemical methods. J. Mol. Liq. 286, 110831. https://doi.org/10.1016/j.molliq.2019.04.108.

Dobrucka, R., Dlugaszewska, J., Kaczmarek, M., 2018. Cytotoxic and antimicrobial effects of biosynthesized ZnO nanoparticles using of *Chelidonium majus* extract. Biomed. Microdevices 20 (1), 5.

Ezealisiji, K.M., Siwe-Noundou, X., Maduelosi, B., Nwachukwu, N., Krause, R.W.M., 2019. Green synthesis of zinc oxide nanoparticles using Solanum torvum (L) leaf extract and evaluation of the toxicological profile of the ZnO nanoparticles–hydrogel composite in Wistar albino rats. Int. Nano Lett. 9 (2), 99–107.

Fahimmunisha, B.A., Ishwarya, R., AlSalhi, M.S., Devanesan, S., Govindarajan, M., Vaseeharan, B., 2020. Green fabrication, characterization and antibacterial potential of zinc oxide nanoparticles using Aloe socotrina leaf extract: a novel drug delivery approach. J. Drug Delivery Sci. Technol. 55, 101465. https://doi.org/10.1016/j.jddst.2019.101465.

Mohammadi, G., Zangeneh, M.M., Zangeneh, A., Siavosh Haghighi, Z.M., 2019. Appl. Organometal. Chem. 33, e5136.

Ghaneialvar, H., Sahebghadam Lotfi, A., Arjmand, S., et al, 2019. Comp. Clin. Path. 28, 1077–1085.

Ghidan, A.Y., Al-Antary, T.M., Awwad, A.M., 2016. Green synthesis of copper oxide nanoparticles using Punica granatum peels extract: effect on green peach Aphid. Environ. Nanotechnol. Monit. Manage. 6, 95–98.

Goorani, S., Koohi, M.K., Morovvati, H., Hassan, J., Ahmeda, A., Zangeneh, M.M., 2020. Appl. Organometal. Chem. 34, e5465.

Harshiny, M., Iswarya, C.N., Matheswaran, M., 2015. Biogenic synthesis of iron nanoparticles using Amaranthus dubius leaf extract as a reducing agent. Powder Technol. 286, 744–749.

Hassanshahian, M., Saadatfar A., Masoumipour F., 2020. Formulation and characterization of nanoemulsion from Alhagi maurorum essential oil and study of its antimicrobial, antibiofilm, and plasmid curing activity against antibiotic-resistant pathogenic bacteria. 2020-08-31. https://doi.org/10.1007/s40201-020-00523-7.

Jalalvand, A.R., Zhaleh, M., Goorani, S., Zangeneh, M.M., Seydi, N., Zangeneh, A., Moradi, R., 2019. Chemical characterization and antioxidant, cytotoxic, antibacterial, and antifungal properties of ethanolic extract of Allium Saralicum RM Fritsch leaves rich in linolenic acid, methyl ester. J. Photochem. Photobiol., B 192, 103–112.

Katata-Seru, L., Moremedi, T., Aremu, O.S., Bahadur, I., 2018. Green synthesis of iron nanoparticles using Moringa oleifera extracts and their applications: removal of nitrate from water and antibacterial activity against Escherichia coli. J. Mol. Liq. 256, 296–304.

Laghari, A.H., Ali Memon, A., Memon, S., Nelofar, A., Khan, K.M., Yasmin, A., 2012. Determination of free phenolic acids and antioxidant capacity of methanolic extracts obtained from leaves and flowers of camel thorn (Alhagi maurorum). Nat. Prod. Res. 26 (2), 173–176.

Laghari, A.H., Memon, S., Nelofar, A., Khan, K.M., 2011. Alhagi maurorum: a convenient source of lupeol. Ind. Crops Prod. 34 (1), 1141–1145.

Chandrasekaran, M., Pandurangan, M., 2016. In vitro selective antiproliferative effect of zinc oxide nanoparticles against co-cultured C2C12 myoblastoma cancer and 3T3-L1 normal cells. Biol. Trace Elem. Res. 172 (1), 148–154.

Zangeneh, M.M., 2019. Appl Organometal Chem. 33, e5295.

Mahdavi, B., Saneei, S., Qorbani, M., Zhaleh, M., Zangeneh, A., Zangeneh, M.M., Pirabbasi, E., Abbasi, N., Ghaneialvar, H., 2019b. Ziziphora clinopodioides Lam leaves aqueous extract mediated synthesis of zinc nanoparticles and their antibacterial, antifungal, cytotoxicity, antioxidant, and cutaneous wound healing properties under in vitro and in vivo conditions. Appl. Organomet. Chem. 33 (11). https://doi.org/10.1002/aoc.v33.1110.1002/aoc.5164.

Mahmoudi, R., Tajali Ardakani, M., Hajipour Verdom, B., Bagheri, A., Mohammad-Beigi, H., Aliakbari, F., Salehpour, Z., Alipour, M., Afrouz, S., Bardania, H., 2019. Chitosan nanoparticles containing Physalis alkekengi-L extract: preparation, optimization and their antioxidant activity. Bull. Mater. Sci. 42 (3). https://doi.org/10.1007/s12034-019-1815-3.

Mao, B.-H., Tsai, J.-C., Chen, C.-W., Yan, S.-J., Wang, Y.-J., 2016. Mechanisms of silver nanoparticle-induced toxicity and important role of autophagy. Nanotoxicology 10 (8), 1021–1040.

Moradi, R., Hajialiani, M., Salmani, S., et al, 2019. Comp. Cli. Path. 28 (5), 1205–1211.

Namvar, F., Rahman, H.S., Mohamad, R., Baharara, J., Mahdavi, M., Amini, E., et al, 2014. Cytotoxic effect of magnetic iron oxide nanoparticles synthesized via seaweed aqueous extract. Int. J. Nanomed. 9, 2479.

Oganesvan, G.B., Galstyan, A.M., Mnatsakanyan, V.A., Paronikyan, R.V., Ter-Zakharyan, Y.Z., 1991. Phenolic and flavonoid compounds of Ziziphora clinopodioides. Chem. Nat. Compd. 27 (2). 247-247.

Pai, S., H, S., Varadavenkatesan, T., Vinayagam, R., Selvaraj, R., 2019. Photocatalytic zinc oxide nanoparticles synthesis using Peltophorum pterocarpum leaf extract and their characterization. Optik 185, 248–255.

Radini, I.A., Hasan, N., Malik, M.A., Khan, Z., 2018. Biosynthesis of iron nanoparticles using Trigonella foenum-graecum seed extract for photocatalytic methyl orange dye degradation and antibacterial applications. J. Photochem. Photobiol., B 183, 154–163.

Rao, M.D., Pennathur, G., 2017. Green synthesis and characterization of cadmium sulphide nanoparticles from Chlamydomonas reinhardtii and their application as photocatalysts. Mater. Res. Bull. 85, 64–73.

Rashidi, K., Mahmoudi, M., Mohammadi, G., et al, 2018. Int. J. Biol. Macromol. 120, 587–595.

Mahmoudi, Reza, Aghaei, Saeed, Salehpour, Zeinab, Mousavizadeh, Ali, Khoramrooz, Seyed Sajjad, Sisakht, Marzie Taheripour,

Christiansen, Baneshi, Marzieh, Karimi, Bahman, Bardania, Hassan, . Antibacterial and antioxidant properties of phyto-synthesized silver nanoparticles using Lavandula stoechas extract. Appl. Organometal. Chem. https://doi.org/10.1002/aoc.5394.

Saha, R., Karthik, S., Balu, K.S., Suriyaprabha, R., Siva, P., Rajendran, V., 2018. Influence of the various synthesis methods on the ZnO nanoparticles property made using the bark extract of Terminalia arjuna. Mater. Chem. Phys. 209, 208–216.

Sangami, S., Manu, B., 2017. Synthesis of Green Iron Nanoparticles using Laterite and their application as a Fenton-like catalyst for the degradation of herbicide Ametryn in water. Environ. Technol. Innovation 8, 150–163.

Sankar, R., Maheswari, R., Karthik, S., Shivashangari, K.S., Ravikumar, V., 2014. Anticancer activity of Ficus religiosa engineered copper oxide nanoparticles. Mater. Sci. Eng., C 44, 234–239.

Seydi, N., Mahdavi, B., Paydarfard, S., Zangeneh, A., Zangeneh, M. M., Najafi, F., et al, 2019. Preparation, characterization, and assessment of cytotoxicity, antioxidant, antibacterial, antifungal, and cutaneous wound healing properties of titanium nanoparticles using aqueous extract of Ziziphora clinopodioides Lam leaves. Appl. Organometal. Chem.

Aman, Shaneza, Gupta, Umesh Kumar, Singh, Deepa, Khan, T., 2018. Herbal treatment for the ovarian cancer. SGVU J. Pharmac. Res. Educ. 3 (2), 325–329.

Sharma, A., Cinti, C., Capobianco, E., 2017. Multitype network-guided target controllability in phenotypically characterized osteosarcoma: role of tumor microenvironment. Front. Immunol. 8, 918.

Sharmila, Govindasamy, Thirumarimurugan, Marimuthu, Muthukumaran, Chandrasekaran, 2019. Green synthesis of ZnO nanoparticles using Tecoma castanifolia leaf extract: characterization and evaluation of its antioxidant, bactericidal and anticancer activities. Microchem. J. 145, 578–587.

Sherkatolabbasieh, H., Hagh-Nazari, L., Shafiezadeh, S., Goodarzi, N., Zangeneh, M.M., Zangeneh, A., 2017. Arch. Biol. Sci. 69 (3), 535–543.

Tahvilian, Reza, Zangeneh, Mohammad Mahdi, Falahi, Homeyra, Sadrjavadi, Komail, Jalalvand, Ali R., Zangeneh, Akram, 2019. Green synthesis and chemical characterization of copper nanoparticles using Allium saralicum leaves and assessment of their cytotoxicity, antioxidant, antimicrobial, and cutaneous wound healing properties. Appl. Organomet. Chem. 33 (12). https://doi.org/10.1002/aoc.v33.1210.1002/aoc.5234.

Sharma, Vyom, Anderson, Diana, Dhawan, Alok, 2012. Zinc oxide nanoparticles induce oxidative DNA damage and ROS-triggered mitochondria mediated apoptosis in human liver cells (HepG2). Apoptosis 17 (8), 852–870.

Zangeneh, Mohammad Mahdi, Bovandi, Shabnam, Gharehyakheh, Sepideh, Zangeneh, Akram, Irani, Parisa, 2019. Green synthesis and chemical characterization of silver nanoparticles obtained using Allium saralicum aqueous extract and survey of in vitro antioxidant, cytotoxic, antibacterial and antifungal properties. Appl. Organomet. Chem. 33 (7). https://doi.org/10.1002/aoc.v33.710.1002/aoc.4961.

Zhaleh, M., Zangeneh, A., Goorani, S., Seydi, N., Zangeneh, M.M., Tahvilian, R., et al, 2019. In vitro and in vivo evaluation of cytotoxicity, antioxidant, antibacterial, antifungal, and cutaneous wound healing properties of gold nanoparticles produced via a green chemistry synthesis using Gundelia tournefortii L. as a capping and reducing agent. Appl. Organometal. Chem. 33 (9).

Zhaleh, M., Sohrabi, N., Zangeneh, M.M., et al, 2018. J Essent Oil Bear Pl. 21 (2), 493–501.